

Scaling quantum probe for quantum phase transition in macroscopic qubit array

Y. D. Wang, Fei Xue, C. P. Sun*

Institute of Theoretical Physics, The Chinese Academy of Sciences, Beijing, 100080, China

(Dated: May 25, 2019)

Based on a superconducting circuit, we discuss the quantum phase transition of a qubit-array quantum Ising model with a quantum probe which is realized by the single mode quantized field in a superconducting transmission line resonator coupled to this qubit array. The scaling behavior of quantum probe near the critical point is analyzed for its quantum coherence. The critical index of decoherence factor is found to be 4.

PACS numbers: 74.81.Fa, 03.65.Fd, 75.10.Pq, 73.43.Nq

Introduction – The nonanalyticity of the ground state energy of an infinite lattice system with respect to a dimensionless parameter λ is referred to as quantum phase transition (QPT) [1]. QPT is essentially caused by quantum fluctuations and implies ultra sensitivity of quantum dynamics near the critical point λ_c . In quantum chaos [2] the sensitivity of perturbations in the Hamiltonian system can also be understood according to the Loschmidt echo (LE) [3]. It was indicated that there exist profound relationship between LE and QPT of an engineered environment [4, 5, 6]. The dynamics of QPT has also been explored [7].

On the other hand the 1D quantum Ising model in the transverse field (the ITF model) [8] is intriguing in demonstrating the critical phenomena in QPT. However, due to the impurities of practical materials, it seems to be very difficult to observe these behaviors in realistic systems. Recently, the superfluid-Mott insulator phase transition was demonstrated in a macroscopic quantum system – the atomic Bose-Einstein condensate in an optical lattice [9]. This experiment and many following search in this direction motivate us to consider the QPT for another macroscopic quantum system – the quantum network formed by superconducting Josephson junction qubits. Numerous efforts have long been devoted to Josephson junction array system to study the Mott insulator-superfluid QPT, e.g. [10] and references therein. Until recently, the research of Josephson junction extended to qubit regime and several superconducting qubit array configurations have been investigated for unpaired Majorana fermion states [11] and quantum state transfer [12, 13].

In this letter, we propose a superconducting qubits array configuration, which can be modeled as an engineered ITF model. The QPT of this model is investigated by a quantum probe which is realized by an on-chip transmission line resonator (TLR) coupled to the qubit array. Examining the decoherence factor of the TLR, the critical behavior of the QPT system is analyzed in detail. The critical index of the quantum probe is found to be 4. This observation suggests that the decoherence has similar property as the thermodynamic quantities (e.g. heat capacity, susceptibility). The experimental feasibility

also briefly discussed. This investigation provides a potentially experimental way to detect QPT in macroscopic Circuit QED as well as enables us to understand the intrinsic relations between QPT and quantum coherence.

Macroscopic QPT model and spectrum structure: We consider a quantum network including many properly biased Cooper pair boxes (see Fig. 1). It can be regarded as an extension of the capacitively coupled two qubits system in a recent experiment [14]. Each Cooper pair box is connected to a dcSQUID with tunable Josephson tunneling energy which is determined by the magnetic flux threading it. With proper bias voltage, the Cooper pair box behaves as a qubit [15] and the network becomes an engineered "spin" chain with N spin-1/2 particles. If the coupling capacitance C_m between two Cooper pair boxes is much smaller than the total capacitance C_Σ connected to each Cooper pair box (e.g. in ref. [14], $C_m/C_\Sigma \approx 0.05$), the total Hamiltonian reads

$$H_0 = h[B_x] \equiv B_x \sum_{\alpha} \sigma_x^{(\alpha)} + B \sum_{\alpha} \sigma_z^{(\alpha)} \sigma_z^{(\alpha+1)} \quad (1)$$

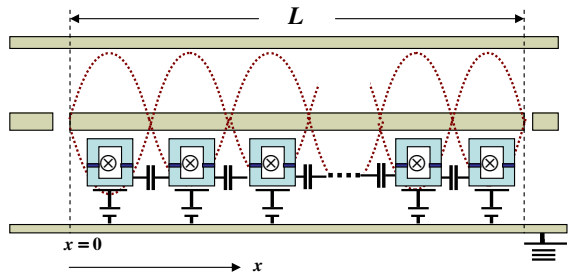


FIG. 1: (Color on line) The schematics of our setup. A capacitively coupled Josephson junction charge qubit array is placed in a 1D transmission line resonator. The qubit array are coupled with the quantized magnetic field of the TLR.

plicity, all qubits are assumed to be identical and biased at the degenerate point. The quasi-spin operators $\sigma_z = |0\rangle\langle 0| - |1\rangle\langle 1|$, $\sigma_x = -|0\rangle\langle 1| - |1\rangle\langle 0|$ are defined with respect to the charge eigenstates, and $|0\rangle$ ($|1\rangle$) denotes 0 (1) Cooper pair state respectively. In general, the Hamiltonian (1) describes QPT in an ideal way. The dimensionless parameter $\lambda \equiv B_x/|B| = 1$ characterizes the competition between the Ising interaction and the transverse field. $\lambda_c = 1$ is a phase transition point from antiferromagnetic state to the paramagnetic gapped state and the energy gap vanishes linearly at the critical point.

In our setup, as a quantum probe, a 1D transmission line is placed near the Josephson junction array (see Fig.1). Each dcSQUID situates at $x = nL/2n_0$ which is the antinode of the quantized magnetic field of the TLR [16] (where n_0 is the mode resonant with the qubits, n is an arbitrary integer and L is the total length of the TLR). Since the electric field vanishes at these points, the qubits are only coupled with the magnetic field. In the single mode case that only one mode a (with frequency ω) of the on-chip resonator couples with the qubits, the magnetic flux in each dcSQUID (with enclosed area S) generated by the single mode is $\phi_x = \eta(a + a^\dagger)$ with $\eta = (S/d)(\hbar\omega/L)^{1/2}$ (d is the distance between the qubit and the transmission line, l the inductance per unit length). Suppose η is small enough for the harmonic approximation [10] $\cos\phi_x \approx 1 - \phi_x^2$, the Hamiltonian for this system is $H = H_0 + H_F$, where

$$H_F = \hbar\omega a^\dagger a - g \sum_{\alpha} (a^\dagger a + a a^\dagger) \sigma_x^{(\alpha)}, \quad (2)$$

with $g = \eta E_J$. Here, we have already invoked the rotation wave approximation to neglect the high frequency terms proportional to $a^\dagger a^\dagger$ and a^2 in the $\omega \gg B_x, B$.

In terms of the subspaces of photon n by n , the above Hamiltonian can be $H = \sum_n H_n |n\rangle\langle n|$ where the branch Hamiltonians $[H_n]$ are defined by Eq.(1) with an external field $\tilde{B}_{nx} = B_x - (2n+1)g$. Here, added a constant term $\hbar n\omega$. Making use of Wigner transformation by $\sigma_x^{(\alpha)} = 1 - \Pi_{\beta < \alpha} (2c_\beta^\dagger c_\beta - 1) (c_\alpha + c_\alpha^\dagger)$ and the diagonalization transformation $c_k = \sum_{\alpha=1}^N c_\alpha \exp(-ik\alpha)/\sqrt{N}$ we can diagonalize H_n as

$$H_n = \sum_k \varepsilon_{nk} \left(\gamma_{nk}^\dagger \gamma_{nk} - \frac{1}{2} \right)$$

Here γ_{nk} is a new set of fermion operators $\gamma_{nk} = \cos(\theta_{nk}/2) c_k - i \sin(\theta_{nk}/2) c_{-k}^\dagger$, $\{\gamma_{nk}, \gamma_{mk'}\} = \delta_{mn} \delta_{kk'}$. The corresponding relation is $\varepsilon_{nk} = 2\sqrt{B^2 + \tilde{B}_{nx}^2 - 2B\tilde{B}_{nx}} \tan\theta_{nk} = -\sin k/(\cos k - \tilde{B}_{nx}/B)$.

Quantum decoherence of the TLR – Let the initial state of the TLR be prepared in a superposed state $|\Psi_{\text{TLR}}(0)\rangle = \sum_n C_n |n\rangle$. Then the state of the ITF model part is driven by different H_n into different branches respectively, i.e., the time evolution of the whole system is described by $|\Psi(t)\rangle = \sum_n C_n |n\rangle e^{-iH_n t} |G\rangle$. Here, the initial state of the ITF part is assumed to be the ground state $|G\rangle$ of the Hamiltonian (1). The decoherence process of the TLR field is represented by the vanishing off-diagonal part of the reduced density matrix which is determined by the decoherence factor

$$D_{mn}(t) = |\langle G | e^{iH_m t} e^{-iH_n t} | G \rangle|^2. \quad (4)$$

This decoherence factor serves as a measure of the coherence of the system. It can be determined by the observation of interference fringe of the quantum field. Another way to evaluate decoherence is based on the so called *purity* $\text{Tr}[\rho_s^2(t)] = \sum_{mn} |C_m C_n|^2 D_{mn}(t)$, which is less than 1 when the quantum system loses part of its quantum coherence. Therefore, the two ways to examine decoherence are essentially the same and our central task is to calculate $D_{mn}(t)$.

To this end we use the Wei-Norman algebraic method [23] to obtain the factorized form of the branch evolution operator $\exp(-iH_n t)$ [18]. After some lengthy but non-trivial calculations, we finally reach

$$D_{mn}(t) \equiv \prod_{k>0} \left(1 - D_k^{(mn)}(t) \right) \quad (5)$$

with $D_k^{(mn)}(t) = \sin^2(\theta_{nk} - \theta_k) \sin^2(\varepsilon_{mk} - \varepsilon_{nk}) t$ and $\tan\theta_k = -\sin k/(\cos k - \lambda)$.

The behavior of the decoherence factor near the critical point is shown in Fig.2. The 3D plot shows the decoherence factor $D_{12}(t)$ as a function of time t and dimensionless parameter λ .

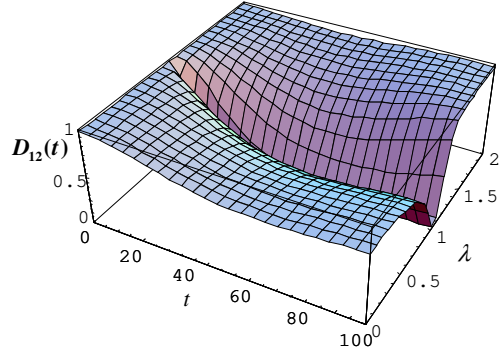


FIG. 2: (Color on line) The 3D diagram of the decoherence factor D_{12} as a function of the time t and the dimensionless parameter λ . Here t is in the unit of $1/B$.

t with $N = 1000$. Fig.3 are a set of diagrams, which are cross sections of $D_{12}(t)$ at a given time t_0 for different N . Both Fig2 and Fig3 reveal one basic feature of the decoherence factor: there is a valley when λ approaches the critical point 1 from both sides. This feature can be directly understood from the expression of H_n . For the case $\lambda \gg 1$, $B_x \gg B \gg g$ so that $B_{nx} \approx B_x$ and the difference between H_n and H_m is negligible. For $\lambda \ll 1$, $B \gg B_x$ and the dominant term in the Hamiltonian is the antiferromagnetic Ising interaction and the transverse field part makes little contribution in determining the quantum state of the system. Therefore the difference between H_m and H_n also tends to be small. It can be found through eq.(4) that the decoherence factor reflects the overlap of different branches under different Hamiltonian. Therefore $D_{mn}(\lambda) \approx 1$ when the two branch Hamiltonians are close to each other. When λ approaches 1, the two competitive terms determine the time evolution in an adjoint way and the difference between H_n and H_m makes significant contribution. Thus, the quantum decoherence caused by the separation of the two branches becomes notable and the deep valley develops. From Fig3, we also find that, as N increases, the decoherence factor is suppressed as a whole since more terms are included in the product (5) and each term is less than 1. This indicates the decoherence effect becomes more prominent as N increases.

Macroscopic QPT and criticality of decoherence – After studying the quantum decoherence in a rather wide range of λ , now we concentrate on the vicinity of the critical point ($|1 - \lambda| \ll 1$) to explore the scaling behavior of

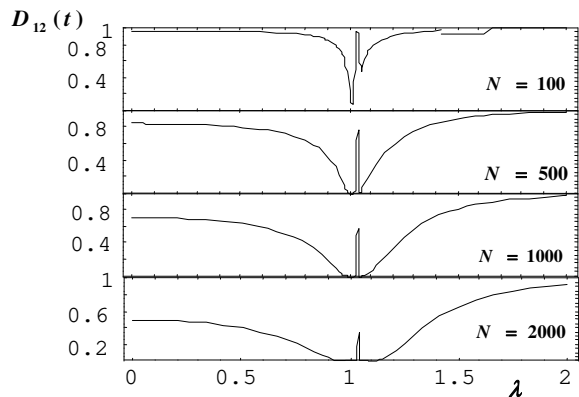


FIG. 3: The decoherence factor of $D_{12}(t)$ for different N as a function of λ at a certain time t_0 that $Bt_0 = 60$. From bottom to top, $N = 2000, 1000, 500, 100$ respectively.

$$g(2n+1) \sin k / (\lambda^2 - 2\lambda \cos k + 1).$$

$W(\lambda, k)$ rapidly decays to zero for large k so that the corresponding $D_k^{(mn)} \ll 1$ term is much smaller than 1. Therefore, only those terms with $k \ll 1$ make contributions to the product eq. (5). With this consideration, we approximately obtain

$$D_k^{(mn)} \approx 8(n-m)^2 (2n+1)^2 \frac{B^2 g^4 k^4 t^2}{(1-\lambda)^4}. \quad (7)$$

According to numerical calculation, in the vicinity of λ_c , $D_k^{(mn)}$ is actually very small in spite of the seemingly divergence. We get $\ln D_{mn}(t) \approx -\sum_k D_k^{(mn)}$. Therefore $D^{(mn)}(t)$ decays exponentially with time, i.e., $D^{(mn)}(t) = \exp(-\gamma_{mn} t^2)$ and the Gaussian decaying rate

$$\gamma_{mn} = 8(n-m)^2 \frac{B^2 g^4 (2n+1)^2}{(1-\lambda)^4} \sum_{k>0} k^4. \quad (8)$$

This is in agreement with Fig.4(a) where the exponential decay behavior of the decoherence factor near the critical point ($\lambda = 1.01$) is plotted according to eq.(5). For a short time duration $t_0 \ll 1/\gamma_{mn}$, $D^{(mn)} \approx 1 - \sum_k D_k^{(mn)}$, the quantum decoherence exhibits an explicit quantum critical behavior around the critical point

$$D_{mn} \sim (1-\lambda)^{-4} \quad (9)$$

where we neglect the "regular" constant 1. Therefore, we get a "critical exponent" -4 for this scaling phenomenon of decoherence factor.

However, it is worthy to point out that this "critical exponent" is different from its conventional counterpart, which is usually defined for the critical behavior of the specific heat, correlation length, etc. This is because the decoherence factor does not diverge at the critical point. Actually, the maximum value for $D_{mn}(t)$ is unity and the above approximation (7) does not hold when λ exactly equals to 1. Nevertheless, this power law behavior is evident as shown in Fig3 although $D_{mn}(t)$ at $\lambda = \lambda_c$ does not diverge. We can see that for each diagram there is a peak at the vicinity of $\lambda = 1$ and as N increases it becomes sharper and lower.

The significance of the critical exponent lies in its universality [19]. The theory based on renormalization group theory suggests that different systems falling into the same universal class have the same critical index. This implies that although we only consider the nearest neighbor interaction in the above discussion, the critical exponent we obtained should be applicable for the much more complicated case when other interactions are also taken into consideration since there is no long range interaction and the two cases belong to the same universal class.

Discussions – In this letter, we present a theoretical scheme based on superconducting circuit to study QPT

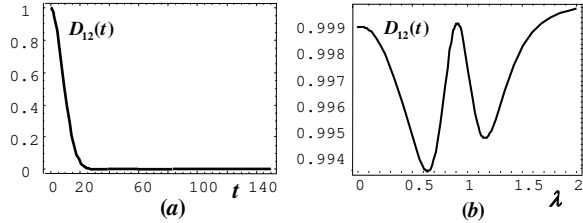


FIG. 4: (a). The exponential decay of the decoherence factor $D_{12}(t)$ with $\lambda = 1.02$, $N = 2000$. Here t is in the unit of $1/B$. (b). The decoherence factor of $D_{12}(t)$ of a 6-qubit array system as a function of λ at a certain time t_0 ($Bt_0 = 60$).

phenomena of a many body quantum system by considering the scaling behavior of the coherence of its quantum probe. Our investigation reveals the profound relationship between QPT and quantum decoherence. The active experimental developments [14, 16] make our model to be potentially feasible in the near future. The main obstacle for experimental realization is the decoherence and dissipation caused by the external environment.

Although in our proposal, all qubits are biased at the degenerate point where the charge fluctuation is largely suppressed, the decoherence and dissipation problem becomes more prominent and may destroy the quantum coherence rapidly when more Cooper pair boxes are included. Therefore, in principle, large number of the spins are extremely difficult to realize. Strictly speaking, QPT happens only at thermodynamic limit that $N \rightarrow \infty$. But some quantum critical phenomena can also be observed for small N [20, 21]. For our proposal, as shown in Fig.4(b), even for small number of qubits, the basic features around the "critical point" is still evident. In this figure, we plot the curves of the decoherence factor for a rather small $N = 6$ system. It can be seen that just as the case with large N , when $\lambda \ll 1$ or $\lambda \gg 1$, the value of the decoherence factor is large; the deep valley develops when λ approaches 1 and there is a peak in the vicinity of the critical point λ_c , i.e., the behavior for small N is quite similar with large N except for the height and width of the valley and peak. The above features imply that, for the experimental realizable small N , the critical phenomenon is still potentially observable.

In order to obtain the analytical result, only the case of $B_z = 0$ is discussed. However, due to the unavoidable charge fluctuation in Josephson junction charge qubit system, It is hard to set the bias charge to $1/2$ precisely. Therefore, more realistic consideration reminds us to extend our present discussion to the case of $B_z \neq 0$. This is the ITF model with longitudinal field. When the longitudinal field is weak enough, the physical property of this model near critical point can be revealed with perturbation theory. Otherwise numerical calculation such as density matrix renormalization group (DMRG) calculation [22] must be utilized for our purpose.

This work is funded by NSFC with grant Nos. 90203018, 10474104, 60433050, and NFRPC with Nos. 2001CB309310 and 2005CB724508.

* Electronic address: suncp@itp.edu.cn;
URL: <http://www.itp.ac.cn/~suncp>

- [1] S. Sachdev, *Quantum Phase Transition*, (Cambridge University Press, Cambridge, 1999).
- [2] A. Peres, *Quantum Theory: Concepts and Methods*, (Kluwer Academic Publishers, Dordrecht, 1995).
- [3] R.A. Jalabert and H.M. Pastawski, Phys. Rev. Lett. **86**, 2490 (2001).
- [4] Z.P. Karkuszewski, C. Jarzynski and W.H. Zurek, Phys. Rev. Lett. **89**, 170405 (2002); F.M. Cucchietti, D.A.R. Dalvit, J.P. Paz and W.H. Zurek, *ibid.* **91**, 210403 (2003).
- [5] C. Emary and T. Brandes, Phys. Rev. Lett. **90**, 044101 (2004).
- [6] H.T. Quan, Z. Song, X.F. Liu, P. Zanardi and C.P. Sun, quant-ph/0509007.
- [7] W.H. Zurek, U. Dorner and P. Zoller, Phys. Rev. Lett. **95** 105701 (2005).
- [8] P. Pfeuty, Ann. Phys. (N.Y.) **57**, 79 (1970).
- [9] M. Greiner, O. Mandel, T. Esslinger, T.W. Hänsch and I. Bloch, Nature **415**, 39 (2002).
- [10] J. Dziarmaga, A. Smerzi, W.H. Zurek and A. R. Bishop, Phys. Rev. Lett. **88**, 167001 (2002).
- [11] L.S. Levitov, T.P. Orlando, J.B. Majer and J.E. Mooij, cond-mat/0108266.
- [12] A. Romito, R. Fazio and C. Bruder, Phys. Rev. B **71**, 100501(R) (2005); A. Lyakhov and C. Bruder, New J. Phys. **7**, 181 (2005).
- [13] M. Paternostro, G.M. Palma, M.S. Kim and G. Falci, Phys. Rev. A **71**, 042311 (2005).
- [14] Y.A. Pashkin *et al.*, Nature **421**, 823 (2003); T. Yamamoto *et al.*, *ibid.* **425**, 941 (2003).
- [15] Y. Nakamura, Yu. A. Pashkin and J. S. Tsai, Nature **398**, 786 (1999).
- [16] A. Wallraff, *et al.*, Nature **431**, 162 (2004); A. Wallraff, *et al.*, Phys. Rev. Lett. **95**, 060501 (2005).
- [17] E. Lieb, T. Schultz and D. Mattis, Ann. Phys. (N. Y.) **16**, 407 (1961).
- [18] The four operators $B \equiv \gamma_{n-k}\gamma_{nk} + \gamma_{n-k}^\dagger\gamma_{nk}^\dagger$, $A \equiv \gamma_{nk}^\dagger\gamma_{nk} \cos^2 \alpha_{mnk} + \gamma_{n-k}^\dagger\gamma_{n-k} \sin^2 \alpha_{mnk}$, $C \equiv B_{nk} - 1$, $D \equiv \gamma_{n-k}^\dagger\gamma_{nk}^\dagger - \gamma_{n-k}\gamma_{nk}$ constitute a close Lie algebra. Then the time evolution derived by the branch Hamiltonian $H_{nk} = A + iB \sin(2(\theta_{nk} - \theta_{nk}))/2$ is written as $U_{nk}(t) = \exp[g_1(t)A]\exp[g_2(t)B]\exp[g_3(t)C]\exp[g_4(t)D]$ according to the Wei-Norman theorem [23] where parameters $g_j(t)$ ($j = 1, 2, 3, 4$) is determined by $i\dot{U}_{nk}U_{nk}^{-1} = H_{nk}$.
- [19] K. Huang, *Statistical Mechanics*, 2nd edition (John Wiley & Sons, 1987).
- [20] X. Peng, J. Du and D. Suter, Phys. Rev. A, **71**, 012307 (2005).
- [21] Y.D. Wang, H.T. Quan, Yu-xi Liu, C.P. Sun and F. Nori, quant-ph/0601026.
- [22] A.A. Ovchinnikov, D.V. Drnitrev, V.Ya. Krivnov and V.O. Cherenovskii, Phys. Rev. B **68**, 214406 (2003).

[23] J. Wei and E. Norman, *J. Math. phys.* **4**, 575 (1963).